Understanding CMUTs with Substrate-Embedded Springs

Byung Chul Lee*, Amin Nikoozadeh, Kwan-Kyu Park, and Butrus (Pierre) T. Khuri-Yakub
Edward L. Ginzton Laboratory, Stanford University, Stanford, CA
*bclee79@stanford.edu

***Abstract* — A capacitive micromachined ultrasonic transducer (CMUT) with substrate-embedded springs, as named post-CMUT or PCMUT, provides many benefits over a conventional CMUT having flexural plate movement. Since the PCMUT structure resembles an ideal piston transducer, the improvements in performance mainly stem from the higher average displacement of the top plate for a given gap height. In this work, comprehensive 3-D finite element analysis (FEA) models are developed to further our understanding of the PCMUT structure. The 3-D FEA models include 3 analysis types, i.e. static, modal, and harmonic analyses, to fully understand the static and dynamic behavior of the PCMUT structure. To reduce the long simulation runtime, simplified 3-D FEA models with quarter symmetry and ideal springs are used instead of full transducer element models. We show that modal analysis results of the 3-D FEA models are in good agreement with the experimental results obtained from the first-generation fabricated PCMUT devices. Two top plate types are considered for the PCMUT structure and hence included in our model: a uniform plate (type 1) and a non-uniform plate (type 2) having a thinner edge portion than its center. Based on the 3-D FEA models, comprehensive parametric simulations were performed for both plate types to understand the effect of each parameter on the static and dynamic behavior. The plate type 2 provided better overall performance than the plate type 1. For the simulated designs the average DC displacement achieved using the plate type 2 was over 50% larger than that for the plate type 1. The FEA simulations also revealed that careful attention must be paid to the engineering of the top plate to assure that unwanted higher plate modes do not interfere with the normal operation of the device within the desired frequency band.**

Keywords- Ultrasound; CMUT; substrate-embedded springs; piston transducer; finite element analysis (FEA)

I. INTRODUCTION

A capacitive micromachined ultrasonic transducer (CMUT) with ideal piston-like plate motion provides many benefits over a conventional CMUT having flexural plate movement [1][2]. As shown in Fig. 1(a) and 1(b), a conventional CMUT is typically composed of multiple cells. Since the anchored regions present in a conventional CMUT structure, the fill factor is less than one, which translates to an inevitable loss in average displacement compared to an ideal piston transducer. While the average plate displacement of an ideal piston transducer is equivalent to its maximum plate displacement, the average displacement of the moving part of a conventional CMUT is typically one third of its maximum plate displacement (Fig. 1(b)). Assuming the same effective gap height, the average displacement of an ideal electrostatic piston transducer is approximately 2.6 times larger than that of the moving part of a conventional CMUT [2][3].

Our proposed CMUT structure with substrate-embedded springs is called post-CMUT or PCMUT because it is composed of a rigid top plate connected to a substrate using long and narrow posts. The posts provide the spring constant of the structure rather than the top plate as in a conventional CMUT (Fig. 1(c)). The PCMUT structure resembles an ideal electrostatic piston transducer, promising improvements in performance by achieving higher average displacement of the top plate for a given gap height.

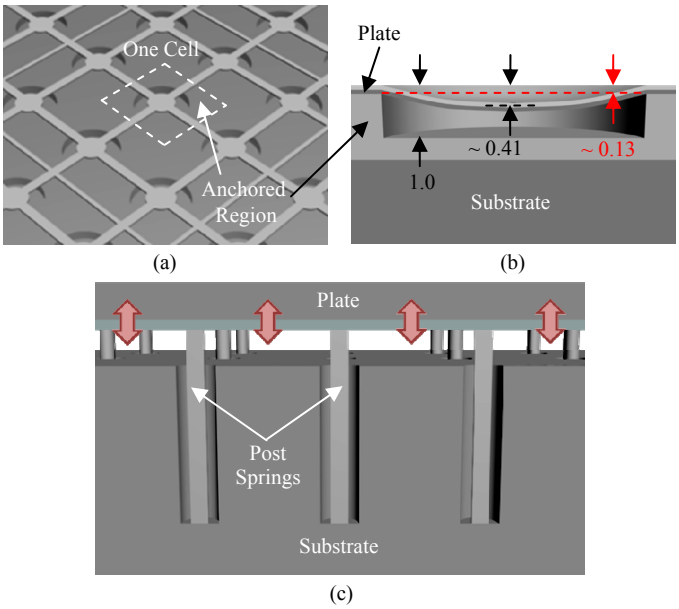

Figure 1. Schematic drawings of (a) a conventional CMUT array, (b) a CMUT cell, and (c) a PCMUT structure

We have previously reported on the PCMUT structure and demonstrated the functionality of the first generation fabricated devices [2]. We measured a peak-to-peak pressure of over 1MPa with a broad fractional bandwidth of over 100%. Our previous FEA model only included simple 2-D structures. Therefore, more complex FEA models involving a whole element representation of the device is desired to better understand the device operation and achieve an optimum design for a particular application.

In this work, we report on comprehensive 3-D FEA models developed to further our understanding of the PCMUT structure. Using these models and the knowledge gained, we present the design considerations required to achieve an optimum design for the PCMUT structure.

II. METHODS

A. 3-D Finite Element Analysis (FEA) Model

We constructed a 3-D FEA full transducer element model as close to a realistic model as possible in order to understand the effect of each parameter on the static and dynamic behavior of the PCMUT structure. We used a commercial tool, ANSYS, Inc. This full transducer element model includes three analysis types: static, modal, and harmonic analyses. In the static analysis, the displacement of the top plate can be simulated for a given DC bias voltage. Additionally, the pull-in voltage of the structure can be automatically calculated. The ideality of the PCMUT structure is also evaluated by the ratio between the average and maximum displacement in the static mode. In the modal analysis, the fundamental and higher harmonic frequencies of a PCMUT structure can be solved for. In the harmonic analysis, an average acoustic pressure spectrum as a function of frequency can be obtained. To realize a practical device, the top plate should provide a complete encapsulation to preserve the vacuum gap, which can be accomplished by anchoring the top plate at the transducer plate edges. We specified two types of top plate: a uniform plate (type 1, Fig. 2(a)) and a non-uniform plate (type 2, Fig. 2(b)) having a thinner edge portion than its center. Due to several resource limitations, such as large number of nodes, long computation time, and limited node and element counts, a simplified 3-D FEA model was constructed. This simplified model assumes a square 2-D array element and it uses a quarter symmetric model for the PCMUT structure and the medium (Fig. 2(c)). The actual posts were also replaced with an ideal spring elements in the simplified model.

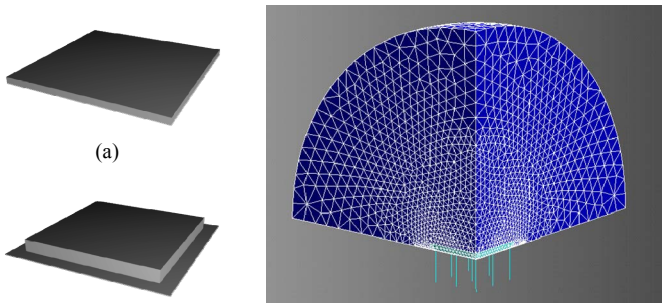

(a) (b) (c)

Figure 2. Schematic illustrations of two PCMUT top plate types: (a) type 1 and (b) type 2. (c) Schematic demonstration of the simplified 3-D FEA model of a PCMUT.

B. Simplified 3-D FEA Model Verification

In order to use the simplified 3-D FEA model instead of a full 3-D FEA transducer element model, it is necessary to compare the simulation results of each model to verify the validity of the simplified model. First, we used FEA to separately model a single post and extract its spring constant. We calculated the error between the values obtained using the theoretical expression for the spring constant and those of FEA simulation results. We confirmed that the error is less than 0.5%. Then, the full 3-D model of a transducer element uses ideal springs with the extracted spring constant in place of the actual posts. The static simulation results between the structures using actual and ideal posts showed minor differences. The error of the average and maximum displacement between them is less than 5%. Thus, the simplified model using the ideal spring elements seems to represent the actual model well.

We used laser doppler vibrometery (LDV) to validate the modal analysis results of the simplified 3-D FEA. It is seen from Fig. 3 that the simulated mode shapes of plate types 1 and 2 show a good agreement with the measurement results. The first mode shape shown for plate type 2 in Fig. 3 is caused by the structural asymmetry due to the electrical connection bridge, which is correctly revealed in the simulation.

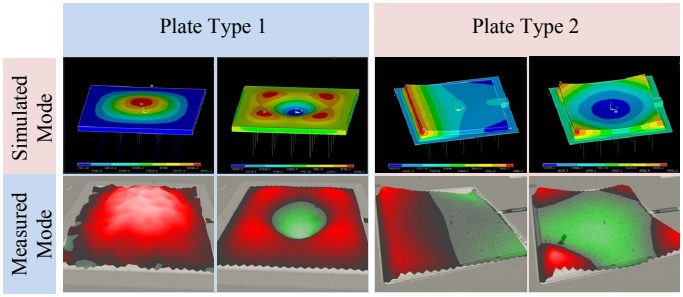

Figure 3. Simulated mode shapes vs. LDV measurements for plate types 1 and 2.

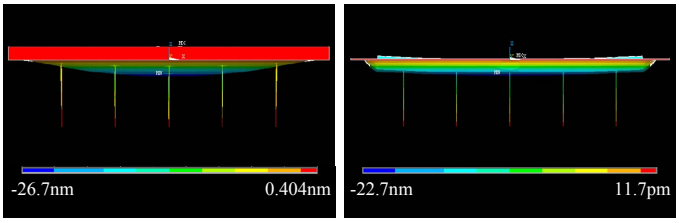

(a) (b)

Figure 4. Static analysis results of plate (a) type 1 and (b) type 2.

C. Analysis of PCMUT Structures

Figure 4 shows the static analysis results for two PCMUT designs, which only differ in their plate types (i.e., one uses plate type 1 and the other plate type 2). For plate type 1 design, the ratio of average to maximum displacement is 0.41, which is close to the conventional CMUT. On the other hand, by making the edge of the top plate thin, as in the plate type 2, the ratio of average to maximum displacement is 0.83, which is closer to the ideal piston transducer. Both the simulations were done at a DC bias equal to 80% of the pull-in voltage for their corresponding design. It is seen from these simulations that the average displacement of the plate type 2 design is approximately twice that of the plate type 1 design.

From the static analysis, we found that the plate type 2 provides better overall performance than the plate type 1. Based on this finding, we started to design a PCMUT structure using plate type 2 for a particular application. We targeted a 2-D array element with a center frequency of about 3.2MHz. Assuming a $\lambda/2$ element pitch criterion at the center frequency, a width of 240μm was determined for the width of the PCMUT element size. Also a fractional bandwidth of about 100% or more was considered as a design target. The physical parameters of a PCMUT design targeting the above specifications are listed in Table 1.

TABLE 1. Simulation Parameters of PCMUT

PARAMETER	VALUE
Number of cells in one element	1
Top plate width (μm)	200
Top plate thickness (μm)	9
Top plate material	Si
Bottom plate width (μm)*	240*
Bottom plate thickness (μm)	1
Bottom plate material	Si
Clamp edge width (μm)	10
Effective gap height (μm)	0.15
Number of posts	25
Post pitch (μm)	40
Post diameter (μm)	5
Post height (μm)	50

* *λ/2 at 3.2 MHz (for phased array)*

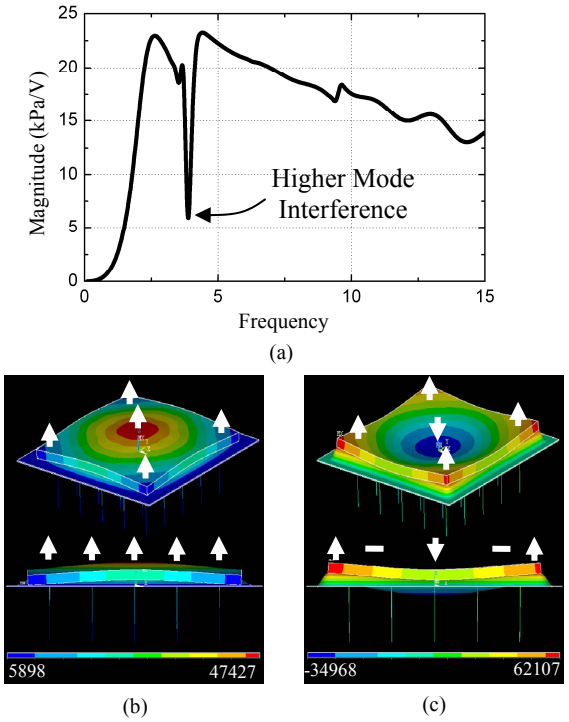

Figure 5. (a) The average acoustic pressure spectrum of the designed PCMUT structure. Modal analysis results of the designed PCMUT structure: (b) Fundamental mode and (c) first undesired higher mode.

Figure 5(a) shows the harmonic analysis result of the designed PCMUT structure. The graph represents an average acoustic pressure over the transducer surface as a function of frequency. As it is seen from this figure, an undesired dip is present in the middle of the frequency band of interest. It turns out that this dip arises from the higher mode interference, which is verified by the modal analysis of the PCMUT structure. Figure 5(b) and 5(c) show the fundamental and the first symmetric harmonic mode shapes of the structure in vacuum. As it is illustrated in these figures, the top plate displacement is in phase at the fundamental frequency of 5.52MHz. However, at the first symmetric harmonic frequency of 6.46MHz, the center and the corners of the top plate are out of phase, resulting in destructive interference. The difference between the fundamental frequency and this undesired harmonic frequency is so close resulting in the appearance of the unwanted dip in the frequency band of interest.

D. Design Consideration of PCMUT

In order to eliminate the undesired dip in the frequency band of interest, the higher mode interference should be outside this range. To this extent, modal analyses were performed with comprehensive parametric changes of the top plate to investigate their effect on this higher mode. Even though not shown here, we observed in our simulations that this undesired mode frequency is mostly a function of the top plate engineering and it is not significantly affected by the existence of the posts. Therefore, for the following modal analyses, only the top plate without any posts was simulated.

First, the Young's modulus of the top plate was modified. As shown in Fig. 6(a), the undesired mode frequency increases when the top plate is stiffer. Choosing an arbitrary Young's modulus that is 100 times that of silicon, we were able to eliminate the unwanted dip in the frequency band of interest and achieve a wide fractional bandwidth of 132% (Fig. 6(b)). This arbitrarily large and maybe unrealistic Young's modulus was primarily chosen to verify that our hypothesis regarding the source of the unwanted dip is indeed valid.

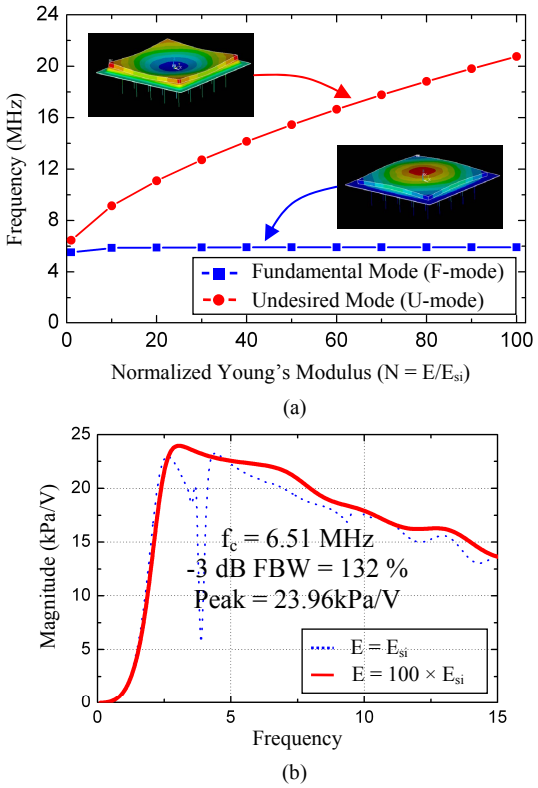

Figure 6. (a) Fundamental and undesired mode frequencies as a function of normalized Young's modulus of the top plate. (b) Average acoustic pressure spectrum showing the effect of large Young's modulus.

There are other ways to achieve a stiffer top plate. The modification of the thickness of the top plate was considered next. As shown in Fig. 7(a), the undesired mode frequency increases when the top plate is thicker. However, a larger thickness contributes to a larger mass so that the fundamental frequency decreases at the same time. We also looked at the effect of shrinking the whole top plate geometry in all dimensions, as seen in Fig. 7(b). In this figure, a "Scaling

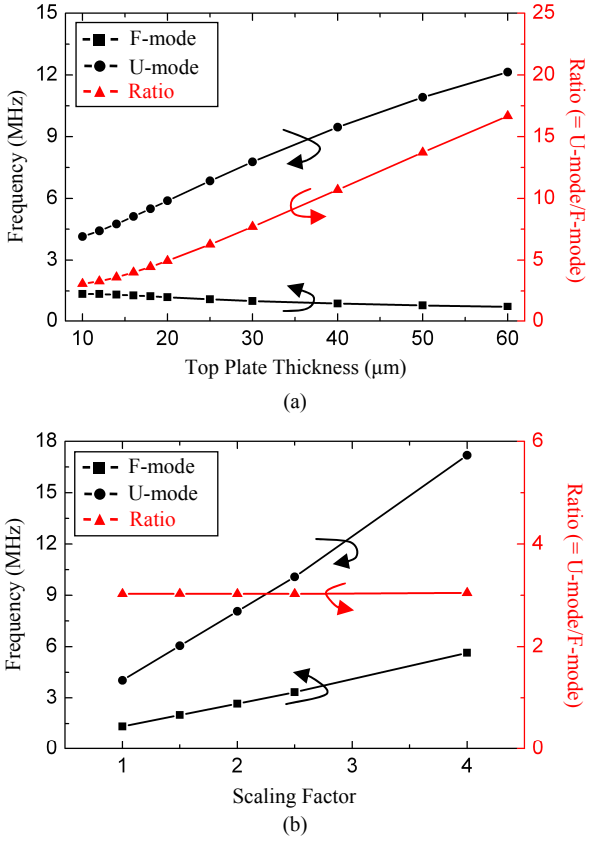

Figure 7. Fundamental and undesired mode frequencies as a function of (a) top plate thickness and (b) scaling factor

Factor" of two, for example, means that all the dimensions (e.g., thickness, width, etc.) of the top plate are linearly shrunk by a factor of two. The fundamental and undesired mode frequencies both linearly increase when the dimensions of the top plate is scaled down.

III. Results and Discussions

Using the knowledge gained in the previous section, we designed a new top plate with its specific dimensions listed in Table 2. In this new design, we mainly scaled the top plate by a factor of 0.5 and also increased the thickness of the top plate to eliminate the higher mode interference, as shown in Fig. 8. However, in this new design, one element is composed of four cells instead of one cell to maintain the same 240μm element pitch. The sharp dip seen in the red plot of Fig. 8, arises from the mutual interaction among cells, which is a well-known phenomenon in conventional CMUT. However, since ANSYS does not take the viscosity of the medium into account in harmonic simulations, this effect may have been unrealistically exaggerated in this simulation. Ignoring this sharp dip, the fractional bandwidth of this new PCMUT design is approximately 100 % around the center frequency of 4.3MHz. Also, the maximum peak pressure is 26.5kPa/V at a frequency of 2.6MHz. All these simulations were performed with a DC bias of 59.5V, which is 80 % of the pull-in voltage.

TABLE 2. Simulation Parameters of modified PCMUT

Parameter	Value
Number of cells in one element	4
Top plate width (μm)	100
Top plate thickness (μm)	20
Top plate material	Si
Bottom plate width (μm)*	120*
Bottom plate thickness (μm)	0.2
Bottom plate material	Si
Clamp edge width (μm)	5
Effective gap height (μm)	0.15
Number of posts	9
Post pitch (μm)	30
Post diameter (μm)	5
Post height (μm)	50

* *λ/4 at 3.2 MHz*

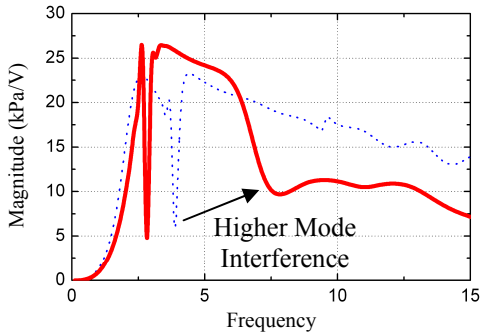

Figure 8. The average acoustic pressure spectrum of the second PCMUT design in table 2.

I. Conclusions and Future Works

We developed a comprehensive 3-D FEA model for the PCMUT structure. Using this model we demonstrated that careful engineering of the top plate is essential in achieving the desired response. In particular, the first harmonic frequency of the top plate should be outside the frequency band of interest to avoid undesired interference.

Based on the simulation results presented here, we will start the fabrication of the second-generation PCMUT devices in the near future.

Acknowledgment

This work was supported by the National Institutes of Health (NIH) under grant 5R01CA134720. We fabricated the PCMUT devices at the Stanford Nanofabrication Facility (Stanford, CA), a member of National Nanotechnology Infrastructure Network. We would like to thank Paul Cristman and Polytec, Inc. for the LDV measurements.

References

[1] Y. Huang, X. Zhuang, E. O. Hæggstrom, A. S. Ergun, C. H. Cheng, and B. T. Khuri-Yakub, "CMUT with piston-shaped membranes: Fabrication and experimental characterization," *IEEE Trans. Ultrason., Ferroelect., Freq. Contr.*, vol. 56, no. 1, pp. 136–145, 2009.

[2] A. Nikoozadeh and B. T. Khuri-Yakub, "CMUT with substrate-embedded springs for non-flexural plate movement," in *Proc. IEEE Ultrason. Symp., San Diego, USA*, pp. 1510–1513, Oct. 2010.

[3] A. Lohfink and P.-C. Eccardt, "Linear and nonlinear equivalent circuit modeling of CMUTs," *IEEE Trans. Ultrason., Ferroelect., Freq. Contr.*, vol. 52, no. 12, pp. 2163–2172, 2005.